ISSN: 2633-4828 Vol. 4 No.2, September, 2022

International Journal of Applied Engineering & Technology

Analysis and determination of solar potential using models based on climatic parameters for the district of San Mateo, province of huarochiri, Lima – Peru

Mendoza Andía, Jhon Américo Rafael; Salvador Gutiérrez, Beatriz Luisa; Sánchez Cortez, Lozano Pedro
Universidad Nacional Mayor de San Marcos, Lima, Perú
(08130130@unmsm.edu.pe); (bsalvadorg@unmsm.edu.pe); (lsanchezc@unmsm.edu.pe)

Date of Submission: 07th May 2022 Revised: 24th September 2022 Accepted:12th October 2022

How to Cite*: Mendoza Andía et.al.,*(2022). Analysis and determination of solar potential using models based on climatic parameters for the district of San Mateo, province of huarochiri, Lima – Peru. International Journal of Applied Engineering &Technology 4(2), pp.87-93.

Abstract: **This paper analyzes a procedure to determine the solar potential through solar radiation estimation models based on climatic parameters, applying them at a local level, where there are no measurement records. The study was carried out in the district of San Mateo, province of Huarochirí, in the highlands of the Lima region, Peru. The use of three estimation models was proposed as calculation alternatives, based on air temperature, since this variable is measured in the vast majority of automatic stations. The use of these models responds to the relationship between temperature and radiation and its practical application, including attenuation due to atmospheric effects. The models used were Bristow-Campbell, Hargreaves-Samani and Annandale, of which the Bristow-Campbell model was selected, which showed better results compared to its peers, obtaining an R^2 of 0.818, RMSE of 1.14, MBE of 0.06 unlike of the R^2 of 0.921 and 0.921, RMSE of 1.27 and 1.27, MBE of -0.52 and -0.52 of Hargreaves-Samani and Annandale respectively.**

To develop the models, a 10-month time series was recorded from its own automatic weather station, complementing the information with a 9-year record of historical data extracted from the free NASA application (POWER) for the auxiliary measurement points located in the whole district. The NASA data were validated by correlating them with the data obtained on the ground giving acceptable results for their application. This made it possible to generate a data log mesh with the measurement points in order to perform the simulation in the free QGIS software and obtain the radiation distribution maps. The annual average radiation was 5.26 kWh/m^{2}day, which is highly profitable.

It is considered that the methodology developed in this research is applicable to estimate the distribution of incident solar radiation at the local level, always considering the conditions of the study area. The global solar radiation values produced in this thesis can be used in the design and performance calculation of solar applications for the San Mateo district.

Keywords: **Solar potential, climatic parameters, Huarochirí**

1. INTRODUCTION

The sun provides energy for most of the processes that occur on the earth's surface. This energy, known as solar radiation, is transferred from the sun in the form of radiant energy that reaches the earth's surface. Solar radiation is the main source of natural energy that plays an irreplaceable role in the energy balance of the Earth-Atmosphere system.

Knowledge of the availability of solar radiation data is of fundamental importance to use solar energy economically and efficiently. In addition to knowing the regions with a high potential to have such use and optimized development. Fortunately, Peru has a general study of solar energy, such information is found in the "Atlas de Energía Solar del Perú", carried out by SENAMHI in conjunction with MINEM, which allows to identify the potential areas with the highest incident solar radiation. However, since this information is general and not specific, it is necessary to quantify the local availability or that of an area of application. This has motivated different studies to be carried out on a more precise scale, which is why this research proposes to determine the solar potential available in the district of San Mateo.

The availability of climate data varies by location, so the method for estimating solar radiation must be adapted to each situation. Data in mountainous terrain regions are often insufficient in terms of coverage and resolution. In this context, solar radiation estimation models become an extremely important issue. There are several methods to estimate solar radiation using different meteorological parameters, such as geographical parameters as latitude, longitude, altitude and meteorological parameters such as air temperature, cloudiness, humidity and sunshine duration

(Almorox, Bocco, & Willington, 2013). For example, the Solar Energy Atlas of Peru (2003), which was formulated based on the Angstrom-Prescott and Bristow-Campbell models, which estimate solar radiation using sunlight duration and air temperature, respectively. This confirms the reliability of the application of the temperature-based models postulated in this research to determine the solar potential available in San Mateo district.

Temperature-based models use the maximum and minimum air temperature to estimate the attenuation due to the effect of the atmosphere. These models assume that the maximum temperature will decrease with reduced transmissivity, while the minimum temperature will increase due to cloud emissivity. In the case of clear skies, the maximum temperature will increase due to increased shortwave radiation, and the minimum temperature will decrease as a result of increased transmissivity; then the difference between the daily maximum and minimum air temperatures becomes an indication of cloudiness (Almorox, Bocco, & Willington, 2013).

According to Bristow & Campbell (1984), the size of the difference between daily maximum and minimum air temperatures depends on the ratio of sensible heat to latent heat. Sensible heat depends on daily incoming solar radiation and is responsible for the maximum air temperatures. At night, sensible heat is lost to space as longwave radiation; together with radiation fluxes, this results in a decrease in air temperature until the daily minimum temperature is reached, usually before sunrise. With this physical clarification, the use of this type of models is justified, with the advantage obtained by the use of a wide network of meteorological stations that allow measurements of extreme daily temperatures.

In this research, three calculation alternatives were considered for the estimation of solar radiation based on the thermal amplitude, which are described below.

2. MODELS AND METHODOLOGY

BRISTOW-CAMPBELL MODEL

Bristow & Campbell (1984) proposed a model for estimating relative incoming solar radiation as a function of the difference between maximum and minimum temperatures ΔT (°C):

$$\frac{H}{H_0} = a_B * [1 - e^{(-b_B * \Delta T^{c_B})}]$$

$$c_B = 2.116 - 0.072\ (T_{max} - T_{min}) + 57.574 * e^{\varphi}$$

$$b_B = 0.107 * {c_B}^{-2.6485}$$

Where H is Global solar radiation [kWh/m^2], H_0 is Extraterrestrial solar radiation [kWh/m^2], T_{max} is Maximum temperature [°C] and T_{min} is Minimum temperature [°C].

Empirical coefficients (a_B, b_B y c_B) have a physical description. The coefficient a_B represents the maximum value of atmospheric transmittance, which is characteristic of a study area, which in turn depends on pollution and elevation. The coefficients b_B (°C−1) and c_B determine the effect of increases in ΔT in the maximum value of atmospheric transmittance (Meza & Varas, 2000).

HARGREAVES MODEL

Hargreaves & Samani (1982) proposed an empirical equation that took the form of a linear regression model between relative incoming solar irradiance and the square root of ΔT:

$$\frac{H}{H_0} = a * (T_{max} - T_{min})^{0.5}$$

Where “a” It is the empirical adjustment coefficient, which represents the atmospheric transmittance, H is Global solar radiation [kWh/m^2], H_0 is Extraterrestrial solar radiation [kWh/m^2], T_{max} is Maximum temperature [°C], T_{min} is Minimum temperature [°C].

ANNANDALE MODEL

The solar radiation estimated by the Annandale model is a modification of the Hargreaves and Samani model, which was corrected for altitude. The coefficient "a" of the H-S model is equal to A*(1+2.7*10-5*Z) (Annandale, Benadé, & Allen, 2002). Annandale's model can be written as follows:

$$\frac{H}{H_0} = A * (1 + 2.7 * 10^{-5} * Z)(T_{max} - T_{min})^{0.5}$$

Where “A” Represents the maximum value of atmospheric transmittance, Z is The height in meters above sea level where the measurement point is located, H is Global solar radiation [kWh/m^2], H_0 is Extraterrestrial solar radiation [kWh/m^2], T_{max} is Maximum temperature [°C], T_{min} is Minimum temperature [°C].

2.1. METEOROLOGICAL DATA

An automatic weather station of the project's own Davis series was used to measure solar irradiance and parameters that allow calculation in the estimation models. This Davis weather station was the main data recording point where measurements were taken and data was collected during a period of approximately 10 months.

2.2. PREDICTION OF WORLDWIDE ENERGY RESOURCES (POWER NASA)

Provides solar and weather data sets from NASA research to support renewable energy studies, energy efficiency construction, and agricultural needs. This application was used for secondary measurement point data (16).

These model- and satellite-based products have been shown to be accurate enough to provide reliable solar and weather resource data in regions where surface measurements are sparse or nonexistent. The products offer two unique features: the data are global and, in general, contiguous in time (Science’s, 2003).

Local historical data was collected for the proposed observation points (primary and secondary) through its study area web application. From its database, records were extracted for the measurement of solar radiation and parameters that allow the calculation in the estimation models.

Fig. 3. Macro location of measurement points.

3. AREA AND DATA

3.1. LOCATION AND WEATHER

The main measurement area is located between UTM WGS-84 coordinates: 374388.36 E and 8689191.78 N, zone 18 South, at an altitude of 4458 m.a.s.l. approximately in San Mateo.

This region has a climate typical of high Andean regions, where the temperature variation is perceived with great difference between day and night. According to SENAMHI, in its Climate Map of Peru, the district of San Mateo corresponds to the semi-frigid rainy climate or also called Tundra, which occurs at altitudes of 3500 - 6000 meters above sea level. This climate is characterized by average annual temperatures of 7°C, average annual rainfall of 700 mm and perpetual snow in the high mountains.

3.2. METEOROLOGICAL STATION DATA

In the measurement period (January - October) an average temperature of 6.72 °C was obtained. Figure 4 shows the temperature variation for the first months until April corresponding to a warm weather in San Mateo, reaching a maximum value of 16.40 °C, recorded on March 16, while the lowest value was -1.91 °C on April 16. On the other hand, it was recorded that in the cold weather months (June - August) the temperature reached a maximum value of 15.53 °C, recorded on June 7 and the lowest value was -3.74 °C on July 14. On the other hand, an average incident radiation of 5.31 kWh/m2day was obtained. Figure 5 shows that the daily variation of radiation has reached a maximum value of 13.52 kWh/m2day, recorded on October 25, while the lowest value was 0.10 kWh/m2day on March 19. The minimum radiation recorded corresponds mostly to the first hours within the range established as sample selection (6 am - 6 pm) for evaluation. Therefore, its variation ranges from 0.1 kWh/m2 to 0.33 kWh/m2 approximately.

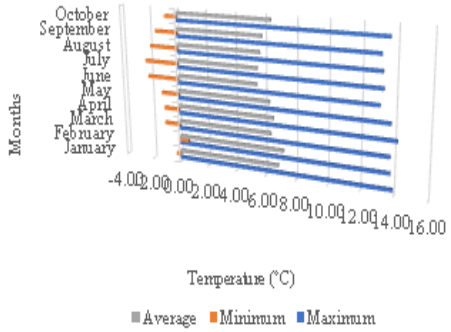

Fig. 4. Monthly average temperature variation.

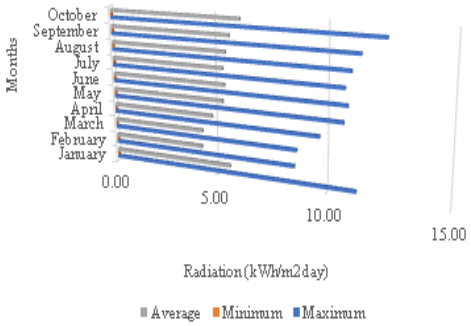

Fig. 5. Monthly average variation of incident radiation.

3.3. PREDICTION OF WORLDWIDE ENERGY RESOURCES (POWER NASA)

An average year was calculated with the values obtained to reflect the temperature variation obtained from the NASA platform. An average temperature of 10.10 °C was obtained. Reaching a maximum average value of 20.74 °C, recorded on April 23; while the lowest average value was -0.67 °C on April 29, corresponding to the warm weather season. Likewise, in the cold weather period, the temperature reached a maximum value of 20.15 °C, recorded on September 21, and the lowest value was -2.82 °C on July 22. On the other hand, an average year was also calculated with the values obtained to reflect the variation of radiation from the NASA platform. An average radiation of 5.13 kWh/m^{2}day was obtained. Reaching a maximum value of 6.59 kWh/m^{2}day, recorded on October 7; while the lowest value was 3.51 kWh/m^{2}day on February 10.

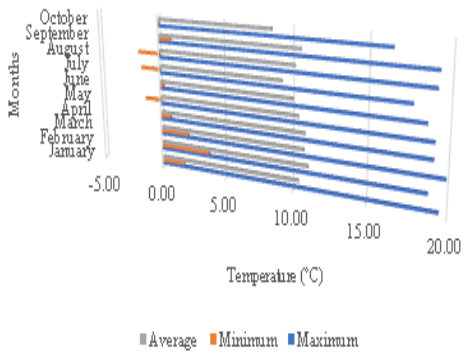

Fig. 5. Monthly average temperature variation.

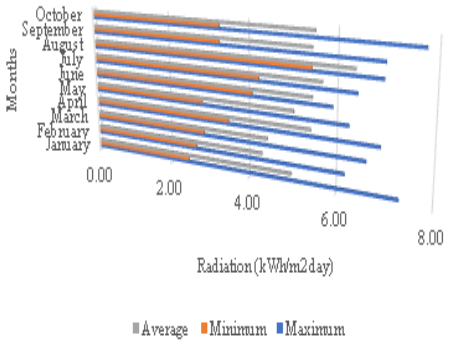

Fig. 6. Monthly average variation of incident radiation.

4. DISCUSSION AND RESULTS

4.1. DATA VALIDATION

In order to visualize the margin of error between the measurements of the WS record and the NASA database during the sampling period (see Table 1), for application at the secondary measurement points, the values obtained were correlated. This data validation process would provide the reliability of the development of the methodology presented in this research.

Table 1. Comparison of recorded MS and NASA values, during the measurement period (2020)

	NASA						Meteorological Station					
	Temperature			Radiation			Temperature			Radiation		
Months	Max	Min	Aver	Max	Min	Aver	Max	Min	Aver	Max	Min	Aver
Jan	19.55	1.75	10.42	7.33	2.48	5.01	16.02	-1.77	7.13	11.25	0.07	5.66
Feb	18.85	3.76	11.09	6.19	2.69	4.32	15.91	-1.31	7.30	8.60	0.07	4.33
Mar	19.90	2.14	10.80	6.64	2.89	4.45	16.40	-1.90	7.25	8.70	0.04	4.37
Apr	19.13	0.74	10.87	6.93	3.51	5.44	16.20	-1.90	7.15	9.69	0.03	4.86
May	19.15	-1.30	10.41	6.27	2.86	5.06	15.95	-2.60	6.68	10.69	0.06	5.38
Jun	18.66	0.25	10.02	5.92	4.09	5.47	15.53	-3.45	6.04	10.93	0.07	5.50
Jul	17.78	-1.57	9.26	6.44	4.25	5.69	14.75	-3.74	5.51	10.73	0.07	5.40
Aug	19.19	-1.76	10.18	6.97	5.46	6.39	15.20	-2.96	6.12	10.98	0.07	5.53
Sep	19.28	0.91	10.57	6.99	3.31	5.47	15.10	-2.69	6.21	11.36	0.07	5.71
Oct	19.48	0.03	8.55	7.77	3.32	5.53	16.10	-2.62	6.74	12.37	0.06	6.21

Source: POWER Data Access NASA & Meteorological station DAVIS.

There is a certain difference between the measurements extracted by satellite and those measured in the field by the MS due to the resolution of the data acquired by satellite. According to NASA, The POWER Project, (2003), the data with which the satellite data is correlated is with the same ground stations. However, the vast majority of the data with which this information is correlated are located in the northern hemisphere. Therefore, it is necessary to verify the information extracted from the POWER application by correlating it with the MS data. A positive correlation of these variables will indicate how closely related they are to each other in order to validate its application at a later date.

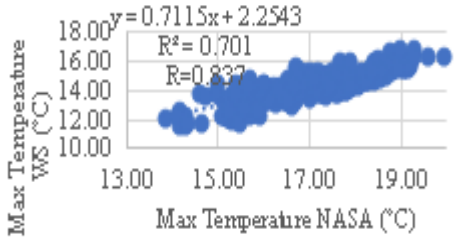

Fig. 7. Correlation of maximum temperature.

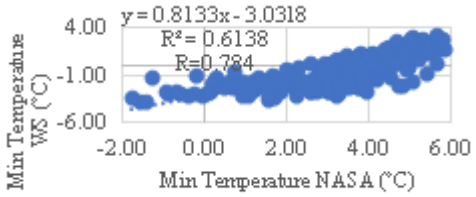

Fig. 8. Correlation of minimum temperature.

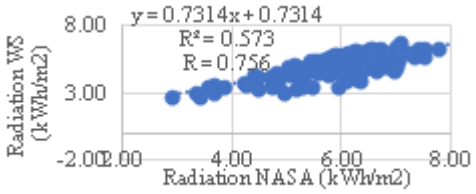

Fig. 9. Correlation of incident radiation.

As shown in Figures 7, 8 and 9, the dispersion of the monthly averages yields a correlation coefficient of 0.88, 0.81 and 0.95, respectively, indicating a positive correlation.

4.2. APPLICATION OF THE PROPOSED ESTIMATION MODELS

Once the recorded data were validated, the calculation of incident solar radiation was carried out using the three alternative estimation models presented, which use thermal amplitude as input parameters, in order to obtain an application methodology for the determination of solar potential with the alternative that shows the best results for the given conditions in the study area.

For the development of each estimation model, the Excel spreadsheet was used, entering the physical and geometric input parameters (location).

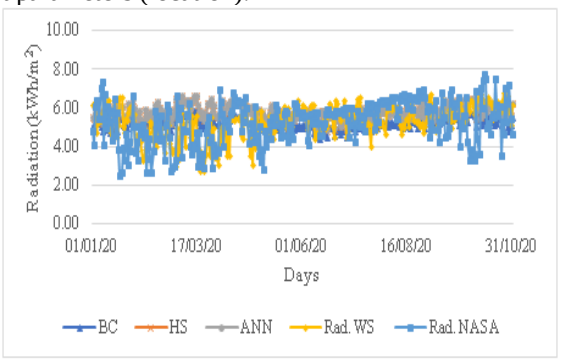

Fig. 10. Incident solar radiation distribution during the measurement period according to each model compared to that obtained from the weather station and the NASA record.

To find the coefficients of the estimation models, the equation was transformed into a linear function form in terms of the parameters that affect the temperature variation. This is done because there is no maximum transmittance parameter (A) in the study area. Therefore, by combining least squares and iteration procedures, the values for the constant are obtained.

Table 2. Comparison of estimated values obtained for each model.

Month	Radiation			
	Measure	Estimated BC	Estimated HS	Estimated ANN
January	5.01	5.20	5.55	5.54
February	4.32	5.21	5.52	5.50
March	4.45	5.51	5.92	5.90
April	5.44	5.39	5.81	5.79
May	5.06	5.05	5.43	5.42
June	5.47	4.90	5.28	5.27
July	5.69	5.03	5.44	5.42
August	6.39	5.24	5.83	5.84
September	5.47	5.40	5.99	5.99
October	5.53	5.38	5.95	5.95

Source: Own elaboration.

4.3. MODEL VALIDATION

Figures 11, 12 and 13 show the dispersion between the measured radiation and the calculated radiation, which allows not only to calculate the atmospheric transmittance constant for the study area, but also allows to determine the level of correlation between these variables and the quality of the model to be used in the results.

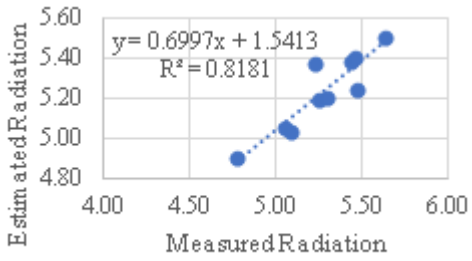

Fig. 11. Correlation of values for the BC model.

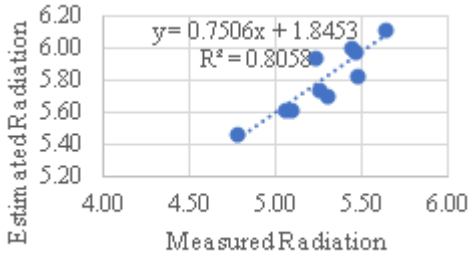

Fig. 12. Correlation of values for the HS model

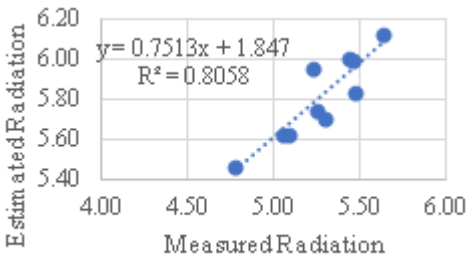

Fig. 13. Correlation of values for the ANN model.

Finally, the analysis of the results ends with a comparison of the recorded values and those calculated by the BC, HS and ANN models. As can be seen in Table 24, the difference between the models is small in percentage terms, which means that for practical purposes and for greater use of solar energy, these differences remain within a margin of reliability considering engineering designs and/or visualization of technology development.

Table 3. Comparative analysis of estimation models using statistical indicators.

Models	Statistical Analysis							
	R2	R	RMSE	MBE	MABE	MPE	MAPE	% Error
Bristow-Campbell	0.904	0.818	1.14	0.06	0.06	-4.30	4.30	1.07
Hargreaves-Samani	0.960	0.921	1.27	-0.52	0.52	-15.66	15.66	-9.77
Annandale	0.960	0.921	1.27	-0.52	0.52	-15.77	15.77	-9.87

Source: Own elaboration.

For the selection of the most optimal model, all the results shown were considered, therefore, to determine the solar potential in the whole district, the one that obtained the most favorable result is selected. In this case, the BS estimation model was the one that obtained the most acceptable values and in accordance with the conditions of the study area, to consider that its application in the auxiliary measurement points is rightly possible, with minimum and simply surmountable errors.

4.4. SPATIAL AND TEMPORAL DISTRIBUTION OF INCIDENT SOLAR RADIATION

The resulting values of the calculated radiation time series of each point (main and secondary) were introduced for the simulation. The modeling was performed by interpolation in the free software QGIS. The number of recording points allows the generation of a mesh with sufficient resources to model the radiation in the annual, monthly and seasonal periods.

Finally, digital maps were obtained showing the ranges of incident radiation distribution with greater precision at the local level (in the study area), considering the effects of climatic variables and the conditions of the area.

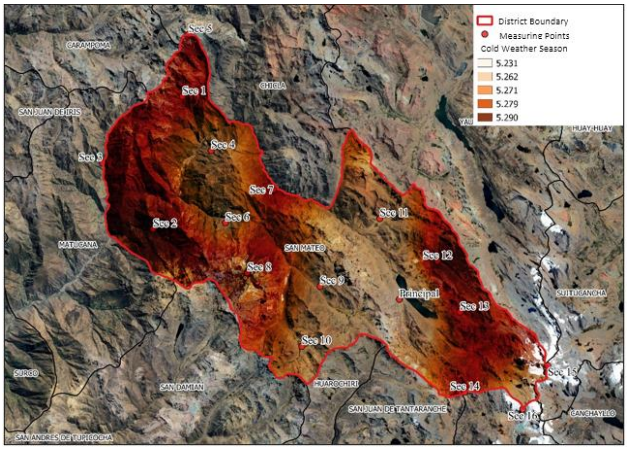

Fig. 14. Annual distribution of incident solar radiation in San Mateo.

The areas where daily solar radiation availability values are recorded are from 5.23 to 5.29 kWh/m^2. These values are within the estimated range for the San Mateo district indicated in the item on profitability.

5. CONCLUSIONS

With the processed data of the maximum and minimum temperatures in the estimation models, the behavior of the incident solar radiation in the study area was determined, in addition to knowing the effect of the variation of these parameters at any time by simply adding the latitude of the site.

The simulation showed that the relationship between the difference between the maximum and minimum temperatures, i.e. the thermal amplitude, depends on the solar radiation that enters daily at dawn and that which is lost at night, generally before dawn. This allows us to use statistical estimation models to determine the solar potential by means of simple climatic parameters of simple registration such as temperature.

The result of this research paper, it is possible to apply the methodology used for the determination of the solar potential at a local level, always verifying the conditions of the study area. Therefore, the conclusions are expressed in two parts:

a) The effect of atmospheric transmittance was determined by relating the measured and calculated radiation in the study area, so that the correlation between both variables gives a constant that avoids the parameterization of the radiative effect of the cloud, and is therefore shown as an indicator of cloudiness for each day of the year to be calculated.

b) The estimation models based on thermal amplitude gave acceptable results, with determination coefficients 0.818, 0.921 and 0.921 for the BS, HS and ANN

models, respectively, with the BS estimation model being the most outstanding and the one that best adapted to the climatic and topographic conditions of the study area. In this sense, it can be affirmed that the use of this type of models for the determination of solar potential in areas where there are no records is presented as a good alternative, but above all viable. The choice of these models is based on the ease of their application, accessible input variables required for their execution and the inclusion of a constant that approximately encompasses the characteristics of atmospheric transmittance.

6. ACKNOWLEDGMENTS

This work was funded by CONCYTEC-FONDECYT within the framework of the call EO41-01 [Contract N ° 156-2018-FONDECYT-BM-IADT-AV] Research project entitled: Development and Implementation of Innovative Technologies with Solar Energy to include the Alpaca Wool Production Chain in the Communities of the San Mateo District, Huarochirí Province.

7. REFERENCES

[1] Almorox, J., Bocco, M., & Willington, E. (2013). Estimation of daily global solar radiation from measured temperatures at Cañada de Luque, Córdoba, Argentina. Renewable Energy, 382-387.

[2] Annandale, J. J., Benadé, N., & Allen, R. (2002). Software for missing data error analysis of Penman-Monteith reference evapotranspiration (Vol. 21(2)). Irrigation Science. doi:10.1007/s002710100047

[3] Bristow, K. L., & Campbell, G. S. (1984). Agricultural and Forest Metereology: On the relationship between incoming solar radiation and daily maximun and minimum temperature (Vol. 31). ELSEVIER. doi:10.1016/0168-1923(84)90017-0

[4] Hargreaves, G. H. (1994). Simplified Coefficients for Estimating Monthly Solar Radiation in North America and Europe. Dept. Biol. And Irrig. Engrg.

[5] Hargreaves, G. H., & Samani, Z. A. (1982). Estimating Potential Evapotranspiration, Journal of the Irrigation and Drainage Division (Vol. 108). Utah, USA: American Society of Civil Engineers, ASCE Library.

[6] Martín, A. M., & Dominguez, J. (2019). Solar Radiation Interpolation. En J. Polo, L. Martin-Pomares, & A. Sanfilippo, Solar Resources Mapping: Fundamentals and Applications (págs. 221-243).

[7] Mendoza Andía, J. A. (2021). Análisis y determinación del potencial solar mediante modelos basados en parámetros climáticos para el distrito de San Mateo, provincia de Huarochirí, Lima – Perú. Obtenido de https://hdl.handle.net/20.500.12672/17413

[8] Ministerio de Energia y Minas, & SENAMHI. (2003). Atlas de energia solar del Perú. Perú: Proyecto PER/98/G31: Electrificacion rural a base de energia fotovoltaica en el Perú.

[9] NASA. (2003). The POWER Project. Obtenido de https://power.larc.nasa.gov/

[10] NASA. (2019). MERRA-2 Modern-Era Retrospective Analysis. Obtenido de Global Modeling and Assimilation Office: https:// gmao.gsfc.nasa.gov/ reanalysis/ MERRA-2/

[11] Soteris A., K. (2014). Solar Energy Engineering, Processes and Systems, Second Edition. ELSEVIER.